

Dielectric relaxations and optical properties of polyvinylidene fluoride/chitosan films

Cite as: AIP Advances 10, 095127 (2020); <https://doi.org/10.1063/5.0022490>

Submitted: 22 July 2020 . Accepted: 31 August 2020 . Published Online: 21 September 2020

S. El-Sayed , Zeinab R. Farag , and S. Saber

COLLECTIONS

Paper published as part of the special topic on [Chemical Physics](#), [Energy, Fluids and Plasmas](#), [Materials Science](#) and [Mathematical Physics](#)



View Online



Export Citation




CrossMark



NEW!

Sign up for topic alerts
New articles delivered to your inbox



Dielectric relaxations and optical properties of polyvinylidene fluoride/chitosan films

Cite as: AIP Advances 10, 095127 (2020); doi: 10.1063/5.0022490

Submitted: 22 July 2020 • Accepted: 31 August 2020 •

Published Online: 21 September 2020



View Online



Export Citation



CrossMark

S. El-Sayed,^{1,a)}  Zeinab R. Farag,²  and S. Saber¹

AFFILIATIONS

¹Department of Physics, Faculty of Science, Fayoum University, 63514 El Fayoum, Egypt

²Department of Chemistry, Faculty of Science, Fayoum University, 63514 El Fayoum, Egypt

^{a)}Author to whom correspondence should be addressed: ssa06@fayoum.edu.eg

ABSTRACT

Polyvinylidene fluoride (PVDF) was blended with different ratios (5%, 7%, and 10% w/w) of chitosan (CS). The dielectric properties of pure PVDF and CS/PVDF films were investigated in (30 °C–140 °C) and (10² Hz–10⁶ Hz) ranges. Both frequency and temperature dependence of the real part, M' , and the imaginary part, M'' , of the dielectric modulus were analyzed. The ac conductivity (σ_{ac}) of all samples was studied to throw light on the conduction mechanism. Results of the UV–vis spectra of the films were discussed to determine important optical parameters when CS is blended with PVDF. There is a good consistency between the dielectric and optical results.

© 2020 Author(s). All article content, except where otherwise noted, is licensed under a Creative Commons Attribution (CC BY) license (<http://creativecommons.org/licenses/by/4.0/>). <https://doi.org/10.1063/5.0022490>

I. INTRODUCTION

The study of polymer blends^{1–5} is interesting because of its low cost and easy processing. In addition, blending polymers enables us to have systems of suitable properties that are significantly different from those of the starting components.

Polyvinylidene fluoride (PVDF) has a semi-crystalline structure and different properties^{6–10} such as dielectric, ferroelectric, piezoelectric, and pyroelectric properties. On the other hand, chitosan (CS) as a biopolymer has attracted significant interest due to its advantages,^{11–14} such as being water-soluble, biodegradable, biocompatible, non-toxic, and abundantly available and having excellent film-forming properties in addition to its biomedical applications.

Many researchers studied the physical properties of different blends either on PVDF or CS.^{1,2,15,16} Chen *et al.*¹ reported on the dielectric properties of polypropylene (PP)/PVDF blends and PP/PVDF/styrene maleic anhydride (SMA) ones. The results showed that PP/PVDF/SMA blends have a high dielectric constant and lower dielectric losses than PP/PVDF. To prepare a mixed matrix membrane, CS was blended with different concentrations (0.5 wt. %, 1 wt. %, 1.5 wt. %, 2 wt. %, and 2.5 wt. %) of PVDF.¹⁵

It was found that the blending of CS increased the hydrophilicity, pore size, surface roughness, and surface free energy of the PVDF membrane. Johns and Nakason¹⁶ studied the dielectric properties of natural tuber (NR)/CS blends. As the CS content increased, more dipoles were incorporated into the blend that affects the dielectric constant, losses, and AC conductivity. The thermal properties of PVDF/polyvinyl alcohol (PVA) were reported,² and the results showed that the effective thermal diffusivity depends on the thermal diffusivity of constituents as well as on their relative volume fraction.

Different blend membranes were obtained¹⁷ based on CS with varied sulfonated polyvinylidene fluoride (SPVDF) by using the casting method. Physico-chemical interaction between SVDF and CS has been suggested. These blends could be used as a polymer membrane for fuel cell applications. Lima *et al.*¹⁸ investigated the dielectric permittivity and DC conductivity of collagen/CS blends. They observed that the collagen and CS might interact to form stable films due to the formation of a polyanion–polycation complex of these polymers. With the addition of CS to collagen, the cations become dominant and, therefore, both the dielectric permittivity and the DC conductivity increased.

The study of the dielectric properties of polymeric materials is important since it provides us with essential knowledge of the polarizing effect and helps promote an understanding of the conductivity behavior of such materials. In addition, the investigation of the optical properties of polymeric materials is essential owing to their applications in optical devices. To our knowledge, there are no reports on the dielectric modulus and optical properties of blending PVDF with different amounts (5%, 7%, and 10% w/w) of CS. Moreover, the distinguished advantages of these two polymers encouraged us to throw light on both the dielectric and optical properties of these films to show any possible applications, if there are any.

II. EXPERIMENTAL

Chitosan (CS) was blended with PVDF at 5%, 7%, and 10% (w/w) concentrations. CS/PVDF films were fabricated by grinding CS for 15 min in a ball mill to obtain smaller particles and subsequent mixing of these particles, in their solid form, with the PVDF dope (w/w) and then suspending the CS/PVDF dope mixture in dimethylformamide (DMF). The suspended dope solutions were then mixed using a magnetic stirrer for 24 h, followed by sonication (1 h) and degassing (1 h) to eliminate the entrapped air bubbles. The mixtures were then poured into a clean glass Petri dish and dried at 60 °C under vacuum for 24 h until a constant weight was obtained. Table I shows the compositions of the prepared samples.

Dielectric measurements were performed over a wide range of frequency using a Hioki (Ueda, Nagano, Japan) model 3532 High Tester LCR, with an accuracy of 10^{-4} pF. The temperature was scanned with a T-type thermocouple of an accuracy of ± 1.0 °C. The dielectric modulus was calculated in terms of the complex electric modulus (M^*), that is defined as the inverse of the complex permittivity (ϵ^*),

$$M^* = M' + iM'' = \frac{1}{\epsilon^*}, \quad (1)$$

$$M^* = \frac{\epsilon'}{\epsilon'^2 + \epsilon''^2} + i \frac{\epsilon''}{\epsilon'^2 + \epsilon''^2}, \quad (2)$$

where M' and M'' are the real and imaginary parts of the dielectric modulus, respectively. The dielectric constant (ϵ') and losses (ϵ'') of each sample were calculated as

$$\epsilon' = \frac{Cd}{\epsilon_0 A}, \quad \epsilon'' = \epsilon' \tan \delta, \quad (3)$$

where C is the capacitance, d is the thickness of the sample, ϵ_0 is the permittivity of vacuum, A is the cross-sectional area of the film, and $\tan \delta$ is the loss tangent. Optical measurements were performed at

TABLE I. The compositions of CS/PVDF prepared films.

Sample (wt. %)	S ₁	S ₂	S ₃	S ₄
PVDF	100	95	93	90
CS	0	5	7	10

room temperature using a Shimadzu UV-3600 UV-VIS-NIR spectrophotometer in the wavelength range 200 nm–900 nm with an accuracy of ± 0.2 nm.

III. RESULTS AND DISCUSSION

A. Dielectric measurements

Both the real part (M') and the imaginary part (M'') representations of the dielectric modulus are a good tool to analyze the dielectric behavior of dielectrics. It is usually noted that the complex permittivity, ϵ^* , becomes high due to carrier transport, space charge accumulation, and electrode polarization. In addition, the dielectric modulus was used to understand the phenomenon of relaxation in dielectric materials in the case of the absence of a well-defined peak in the dielectric losses, ϵ'' . To remove electrode polarization of the studied samples and throw light on the relaxation process and conduction mechanism, both frequency and temperature dependence of M' and M'' and ac conductivity, σ_{ac} , have been studied as follows.

B. Frequency dependence

Figures 1(a)–1(d) depict the variation in the real dielectric modulus, M' , vs the frequency, f , at different temperatures for pure PVDF and CS/PVDF films. As seen, the values of M' changed with increasing f due to the charge carriers of short-range mobility. The values of M' tend to zero at low frequency, indicating the removal of electrode polarization. It is also observed that M' of pure PVDF increased by blending with CS. The s-shape of M' is a characteristic trend of the ionic mechanism.¹⁹ One noticed that there is dispersion in M' of all the studied samples around 1.0 kHz. This dispersion could be attributed to the relaxation process around such frequency, as shown in Fig. 2.

The frequency dependence of M'' for PVDF and some CS/PVDF films at some selected temperatures is represented in Figs. 2(a)–2(d). A peak is observed for all samples around 1.0 kHz due to Maxwell–Wagner–Sillars (MWS) interfacial polarization.²⁰ This peak is shifted to a higher frequency with increasing temperature. The position of this peak is determined to estimate the activation energy (E_r) of this relaxation process as

$$\tau = \tau_0 \exp\left(\frac{E_r}{KT}\right), \quad (4)$$

where τ_0 is the limit of the relaxation time at high temperatures and K is Boltzmann's constant.

Figure 3 displays the plot of $\log(\tau)$ vs $1000/T$. The slopes of these lines express the values of E_r (see Table II). The evidence that the relaxation process is MWS interfacial polarization in type is the value of the relaxation time (τ) in addition to the value of $\tau_0 \approx 10^{-13}$ s.²¹ As seen, the values of E_r are less than 1.0, similar to those of the activation energy E_a , (see Fig. 9), which has been determined from the ac conductivity, σ_{ac} , which is temperature-dependent. This result reflects the existence of a hopping mechanism that can be attributed to mainly electronic and partially ionic conduction.²²

The frequency dependence of the ac conductivity (σ_{ac}) at different temperatures for some selected CS/PVDF films is displayed, for

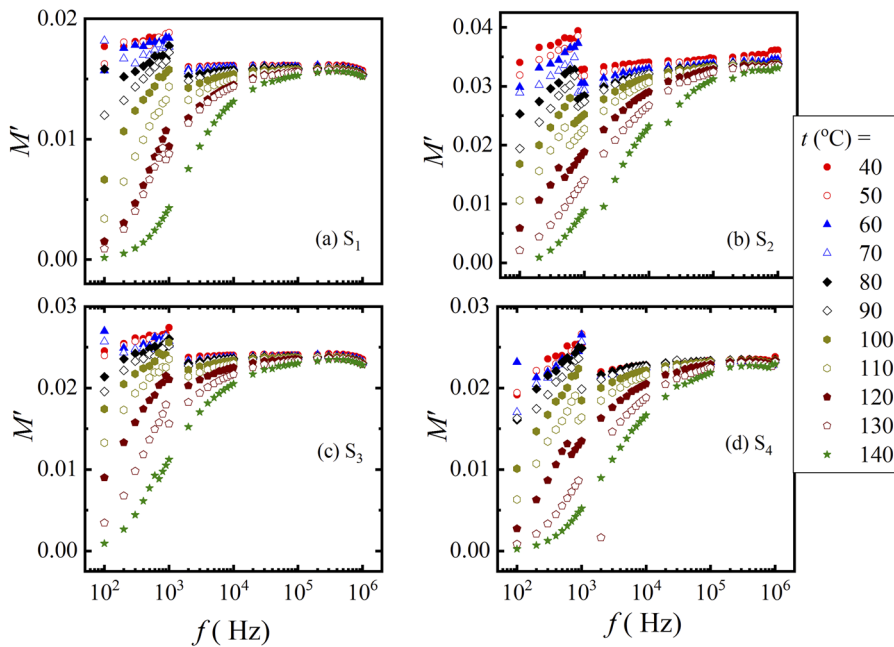


FIG. 1. [(a)–(d)] Frequency dependence of M' on pure PVDF and CS/PVDF films at different temperatures.

instance, in Figs. 4(a) and 4(b). As seen, σ_{ac} increased with increasing f . It was observed that the σ_{ac} of all investigated samples could be described by^{23,24}

$$\sigma_{ac}(\omega) = \sigma_t - \sigma_{dc} \approx A\omega^s, \quad (5)$$

where ω is the angular frequency, σ_t is the total ac conductivity, σ_{dc} is the low-frequency conductivity, A is constant, and s is the exponent factor. As seen, σ_{ac} increases with increasing frequency and temperature. It is noticed that the conduction mechanism is hopping for all studied samples. The s values were calculated from the slope of $\log(\sigma_{ac})$ vs $\log(\omega)$.

The dependence of the frequency exponent, s , on temperature for some films is shown in the upper panel of Fig. 5. The values of s decreased with increasing temperature. Hence, it can be suggested that the correlated barrier hopping conductivity (CBH) is suitable to describe the conduction mechanism. In the CBH model, the exponent s is related to the binding energy of the carriers, W_M , as^{4,25,26}

$$s = 1 - 6kT/W_M, \quad (6)$$

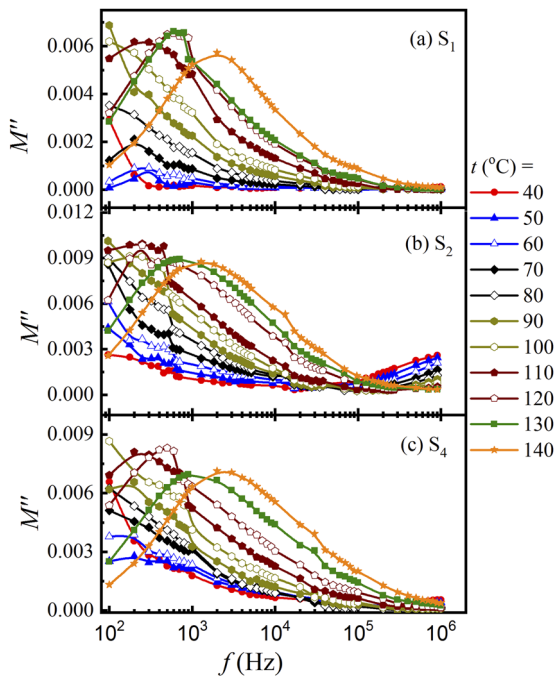


FIG. 2. [(a)–(c)] Frequency dependence of M'' on pure PVDF and CS/PVDF films at different temperatures.

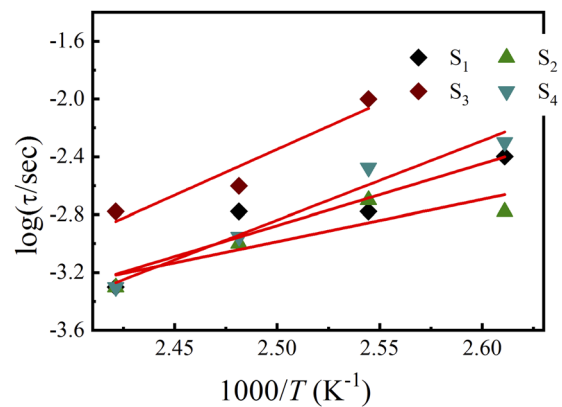


FIG. 3. Change in the relaxation time, τ , against temperature for pure PVDF and CS/PVDF films.

TABLE II. The dielectric and optical parameters of pure PVDF and CS/PVDF blends: the relaxation activation energy (E_r), the binding energy of the carriers (W_M), the indirect energy bandgap (E_g), and the Urbach energy (E_U).

Blend sample	E_r (eV)	W_M (eV)	E_g (eV)	E_U (eV)
S ₁	0.368	0.082	4.0	0.67
S ₂	0.252	0.084	4.3	0.53
S ₃	0.546	0.146	3.7	0.52
S ₄	0.473	0.220	3.6	0.49

where k is Boltzmann's constant and T is temperature. The W_M values were calculated from the slope of $(1 - s)$ against T (see the lower panel of Fig. 5). The calculated values are listed in Table II. One can notice that W_M increased with an increasing CS content.

C. Temperature dependence

Figures 6(a)–6(d) displays the temperature dependence of M' of pure PVDF and some CS/PVDF samples at some selected frequencies. It is observed that the values of M' for all films decreased with increasing temperature while it increased with increasing frequency. At low frequency, M' tends to reach a small value, reflecting the removal of the electrode polarization. In addition, M' reaches constant values at higher temperatures and frequencies owing to the thermally activated behavior of dielectric materials.^{27–29}

The temperature dependence of M'' for all samples is shown in Figs. 7(a)–7(d). An asymmetric peak is observed, which shifted

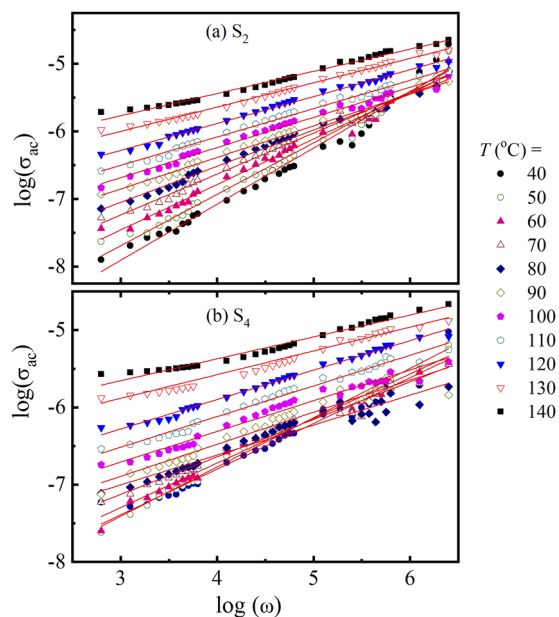


FIG. 4. [(a) and (b)] Frequency dependence of the ac conductivity, σ_{ac} , for (a) S₂ and (b) S₄ at different temperatures. The solid red lines represent the fitting, according to Eq. (5).

toward higher temperatures with increasing frequency for the investigated films. The broadening of this peak reveals the spread of the relaxation times so that the type of such relaxation is non-Debye. More evidence that the type of relaxation is due to MWS polarization is that the intensity of such a peak increases at low frequency and shifts to a higher temperature as the frequency increased.

It is important to throw light on the nature of the conduction mechanism; Figs. 8(a)–8(d) represent the variation in the σ_{ac} of all samples vs $1000/T$. As the temperature increases, σ_{ac} increases because the mobility of the chain segments becomes soft to move and the side groups of the polymers become easy to rotate. In addition, increasing the temperature allows the free charges to hop from one site to another, leading to an increase in the value of σ_{ac} .³⁰ Based on the Arrhenius relation, the behavior of $\sigma_{ac}(T)$ for all investigated samples is described within the temperature ($343 \text{ K} \leq T \leq 413 \text{ K}$) as

$$\sigma_{ac} = \sigma_o \exp\left(-\frac{E_a}{kT}\right), \quad (7)$$

where both k and T have their usual meaning. σ_o is the pre-exponential factor, and E_a is the activation energy.

The thermally activated energy, E_a , was calculated at different frequencies and is presented in Fig. 9. As can be seen from this figure, the value of E_a decreased with increasing frequency and varied from 0.1 eV to 0.3 eV with increasing frequency and within the temperature range ($343 \text{ K} \leq T \leq 413 \text{ K}$).

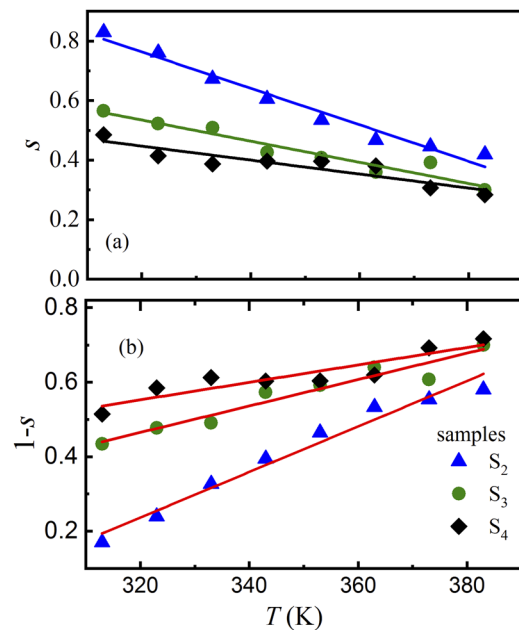


FIG. 5. [(a) and (b)] Upper panel shows the temperature dependence of the frequency exponent, s , for pure PVDF and CS/PVDF films. The lower panel displays the variation in $(1 - s)$ vs the temperature of the investigated samples. The solid red lines in the lower panel show fitting, based on Eq. (6).

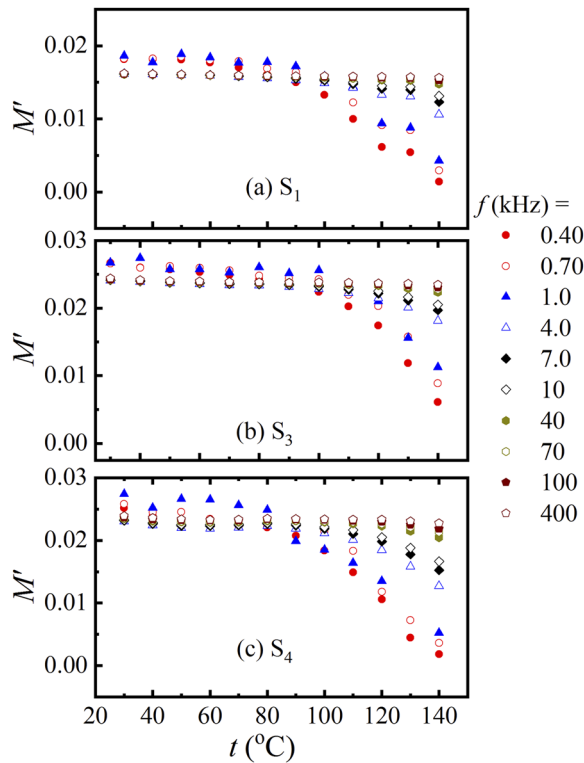


FIG. 6. [(a)–(c)] Temperature dependence of M' on pure PVDF and CS/PVDF films at different frequencies.

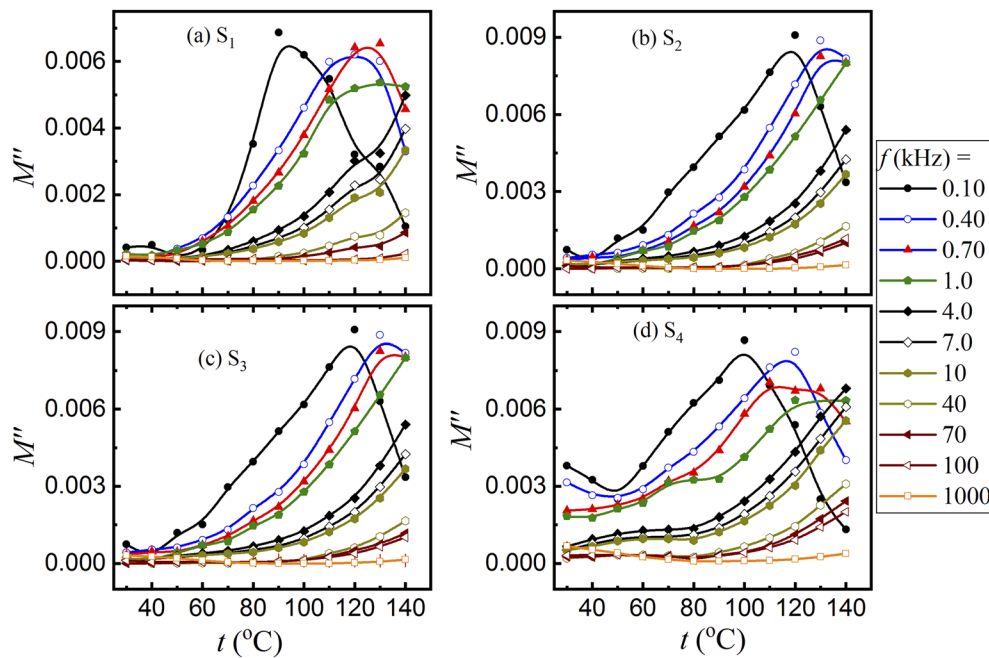


FIG. 7. [(a)–(d)] Temperature dependence of M'' on pure PVDF and CS/PVDF films at different frequencies.

D. Optical properties

UV–vis absorption spectroscopy was used to test the blending of PVDF with CS. Both the absorbance spectra and extinction coefficient (k) of pure PVDF and CS/PVDF films are shown in Figs. 10(a) and 10(b). Above 300 nm, both S_3 and S_4 samples exhibit higher absorbance and k than pure PVDF. On the other hand, S_2 shows lower absorbance and k than PVDF. A clear band of transition was observed in both the absorbance and the k for pure PVDF and CS/PVDF films around 270 nm. This band could be attributed to the π – π^* transition similar to that reported for different polymers.^{31,32}

According to the UV–vis spectra, the indirect optical energy bandgap (E_g) can be estimated by using the following expression:^{33,34}

$$(\alpha h\nu)^{1/2} = \beta(h\nu - E_g), \tag{8}$$

where β is a constant and E_g is the indirect bandgap transitions. The plot of $(\alpha h\nu)^{1/2}$ against $h\nu$ at room temperature enables us to estimate the values of E_g by extrapolating the linear part of $(\alpha h\nu)^{1/2}$ to zero, as displayed in Fig. 11. The obtained E_g values are listed in Table II.

The dependence of the absorption coefficient, α , on $h\nu$ verifies the Urbach relation,³⁵

$$\ln(\alpha) = \ln(\alpha_0) + \frac{h\nu - r}{E_U}, \tag{9}$$

where E_U is the Urbach energy and r and α_0 are constants. The values of E_U were taken from the slopes of the straight lines, as seen in Fig. 12, and are given in Table II. As can be seen in Table II, the E_U values decreased with an increasing blending ratio

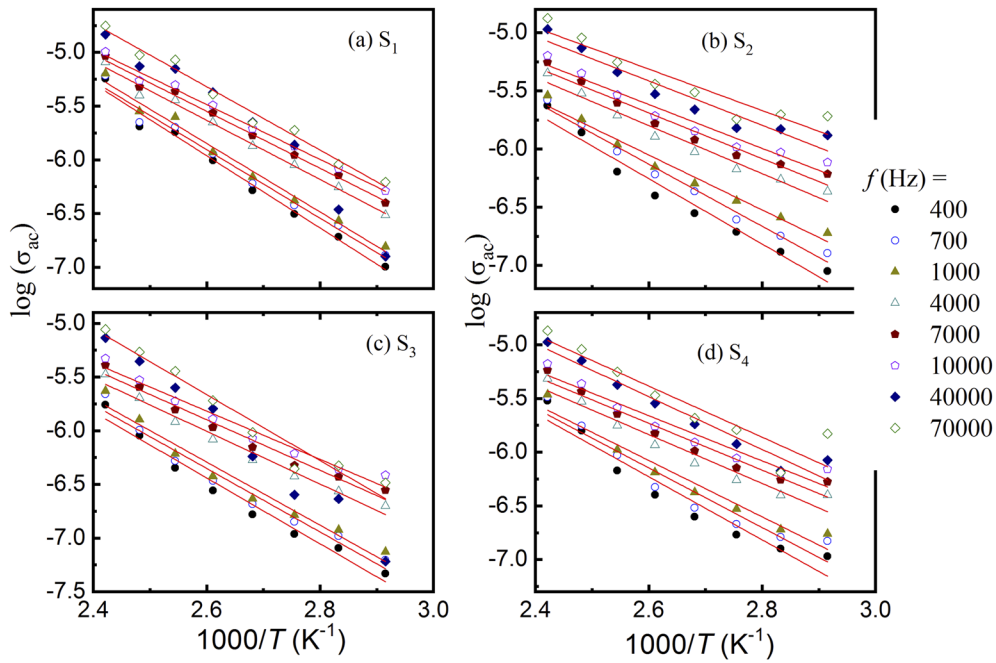


FIG. 8. [(a)–(d)] Temperature dependence of the ac conductivity, σ_{ac} , on pure PVDF and CS/PVDF films at some selected frequencies. The solid red lines display the fitting, according to Eq. (7).

of CS into PVDF in contrast to the trends of E_r . On the other hand, the trend of changing E_U is similar to that of E_a (see Fig. 9) and E_g (see Table II) except for the S_2 sample. The decrease in E_U with blending CS with PVDF may reflect the redistribution of optic states, allowing a large number of possible transitions, either tail-to-tail or band-to-tail. Generally, the change in the values of both E_U and E_g of PVDF with an increasing CS content could be attributed to the same mechanism. This means that adding CS to PVDF increases the charge carriers and the optical transitions.

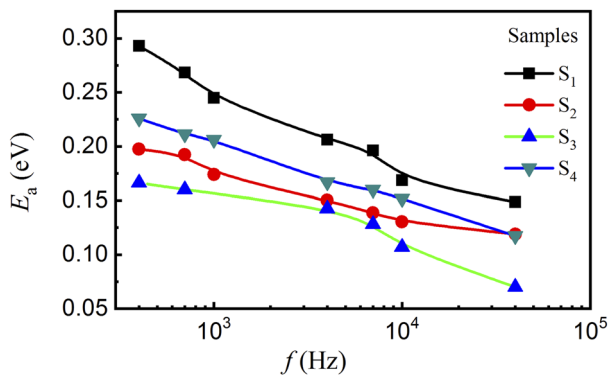


FIG. 9. Variation in the thermal activation energy, E_a , vs frequency for both PVDF and CS/PVDF films.

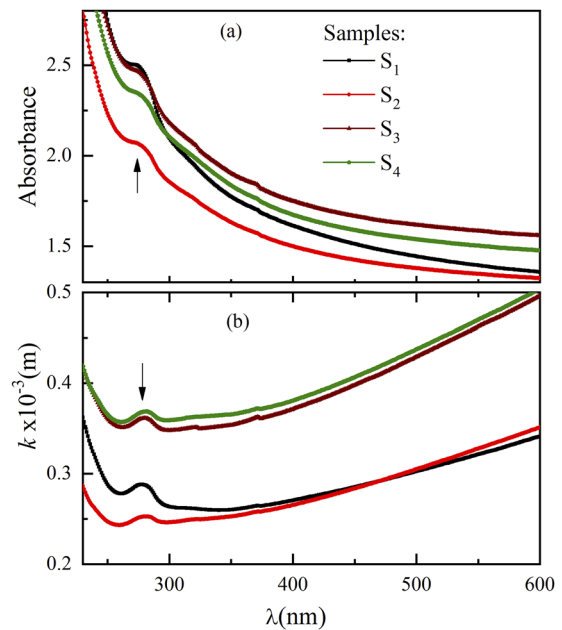


FIG. 10. [(a) and (b)] Upper panel (a) shows the absorbance of the UV-vis of the studied samples while the lower panel (b) presents the change in the extinction coefficient, k , with the wavelength of the investigated films.

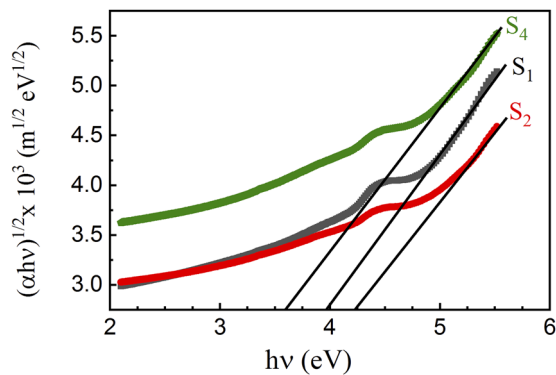


FIG. 11. Plots of $(\alpha hv)^{1/2}$ vs $h\nu$ for pure PVDF and CS/PVDF films.

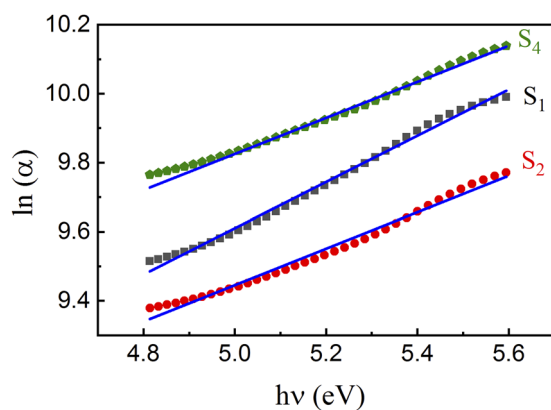


FIG. 12. Change in the absorption coefficient against $h\nu$ to determine the Urbach energy gap of pure PVDF and some selected CS/PVDF films. The solid blue lines show the fitting, according to Eq. (9).

Besides, the variation in the E_r values of the PVDF matrix is irregular with the blending of CS. In addition, decreasing E_g and increasing σ_{ac} indicated good consistency between both dielectric and optical results.

IV. CONCLUSIONS

We succeeded in blending PVDF with different amounts of CS (5%, 7%, and 10% w/w). The dielectric results revealed that the real part of the dielectric modulus, M' , increased with blending CS with PVDF. On the other hand, the imaginary part of the dielectric modulus, M'' , showed a relaxation process that can be attributed to MWS interfacial polarization. The value of the relaxation time is consistent with this type of relaxation. The relaxation activation energy, E_r , is less than 1.0 eV and depends on the amount of CS. The frequency dependence of the ac conductivity, σ_{ac} , was described according to the frequency exponent law ($\approx \omega^s$), where the values of s decreased with increasing temperature and decreased with an increasing CS content. The correlated barrier hopping, CBH, is the conduction mechanism for all the investigated samples. In addition, the temperature dependence of the σ_{ac} of the samples is thermally activated with the activation energy, $E_a < 0.50$ eV. The E_a value of PVDF

decreased by adding CS and may indicate that the conduction is mainly electronic and partially ionic.

The optical absorbance and extinction coefficient, k , showed a band transition around 270 nm due to $\pi-\pi^*$ transition. At $\lambda > 350$ nm, both the absorbance and the k of PVDF increased with CS except for sample S_2 . The indirect bandgap transition, E_g , was calculated using Tauc's relation and found that E_g of PVDF decreased with increasing CS except for S_2 . In addition, the Urbach energy, E_U , was calculated based on UV-vis spectra. It was noted that E_U of PVDF was regularly decreased by adding CS to PVDF. The results of this work indicate a better consistency between the optical and dielectric properties of CS/PVDF films. Finally, the enhancement of either dielectric or optical properties of blending CS to PVDF may improve its performance for suitable applications.

ACKNOWLEDGMENTS

The authors would like to thank Dr. A. Hassen, Professor of Materials Science, Physics Department, Dean of the Faculty of Science, Fayoum University, 63514 El Fayoum, Egypt, for his constant support and useful discussions while performing this work.

DATA AVAILABILITY

The data that support the findings of this study are available from the corresponding author upon reasonable request.

REFERENCES

- Z. Chen, J. Pei, and R. Li, *Appl. Sci.* **7**, 389 (2017).
- G. K. Bama, P. I. Devi, and K. Ramachandran, *J. Mater. Sci.* **44**, 1302 (2009).
- D. M. G. Cruz, J. L. G. Ribelles, and M. S. Sánchez, *J. Biomed. Mater. Res., Part B* **85B**, 303 (2008).
- S. El-Sayed, K. H. Mahmoud, A. A. Fatah, and A. Hassen, *Physica B* **406**, 4068 (2011).
- R. Gregono, M. Cestori, and N. Chaves, *The Polymeric Material Encyclopedia* (CRC Press, Boca Raton, FL, 1996).
- L.-P. Cheng, D.-J. Lin, C.-H. Shih, A.-H. Dwan, and C. C. Gryte, *J. Polym. Sci.* **37**, 2079 (1999).
- K. M. Kim, N.-G. Park, K. S. Ryu, and S. H. Chang, *Polymer* **43**, 3951 (2002).
- A. Tawansi, A. H. Oraby, E. Ahmed, E. M. Abdelrazek, and M. Abdelaziz, *J. Appl. Polym. Sci.* **70**, 1759 (1998).
- N. Jahan, F. Mighri, D. Rodrigue, and A. Ajji, *Appl. Clay Sci.* **152**, 93 (2018).
- L. Bovey, *Phys. Technol.* **18**, 91 (1987).
- N. A. N. Aziz, N. K. Idris, and M. I. N. Isa, *Int. J. Polym. Anal. Charact.* **15**, 319 (2010).
- D. Dutta, G. Das, and V. S. Tripathi, *J. Sci. Ind. Res.* **63**, 20 (2004), available at <http://nopr.niscair.res.in/handle/123456789/5397>.
- M. A. Brown, M. R. Daya, and J. A. Worley, *J. Emerg. Med.* **37**(1), 1 (2009).
- A. A. Aldana, R. Toselli, M. C. Strumia, and M. Martinelli, *J. Mater. Chem.* **22**, 22670 (2012).
- C. N. B. Elizalde, S. Al-Gharabli, J. Kujawa, M. Mavukkandy, S. W. Hasan, and H. A. Arafat, *Sep. Purif. Technol.* **190**, 68 (2018).
- J. Johns and C. Nakason, *J. Non-Cryst. Solids* **357**, 1816 (2011).
- V. Vijayalekshmi and D. Khastgir, *Cellulose* **25**, 661 (2018).
- C. G. A. Lima, R. S. de Oliveira, S. D. Figueiró, C. F. Wehmann, J. C. Góes, and A. S. B. Sombra, *Mater. Chem. Phys.* **99**, 284 (2006).
- M. F. Mostafa and A. Hassen, *Phase Transitions* **79**(4-5), 305 (2006).
- M. Samet, A. Kallel, and A. Sergei, *J. Appl. Polym. Sci.* **136**, 47551 (2019).

- ²¹H. Hammami, M. Arous, M. Lagache, and A. Kallel, *J. Alloys Compd.* **430**, 1 (2007).
- ²²T. A. Hanafy, K. Elbanna, S. El-Sayed, and A. Hassen, *J. Appl. Polym. Sci.* **121**, 3306 (2011).
- ²³A. M. Saleh, R. D. Gould, and A. K. Hassan, *Phys. Status Solidi A* **139**(2), 379 (1993).
- ²⁴R. Bahri and H. P. Singh, *Thin Solid Films* **62**, 291 (1979).
- ²⁵S. R. Elliott, *Adv. Phys.* **36**, 135 (1987).
- ²⁶T. A. Hanafy, *J. Appl. Polym. Sci.* **108**, 2540 (2008).
- ²⁷A. K. Jonscher, *J. Phys. D: Appl. Phys.* **32**, R57 (1999).
- ²⁸T. Abdel-Baset, M. Elzayat, and S. Mahrous, *Int. J. Polym. Sci.* **2016**, 1707018-1–1707018-13.
- ²⁹A. K. Jonscher, *Dielectric Relaxation in Solids* (Chelsea Dielectric, London, UK, 1983).
- ³⁰T. A. Abdel-Baset and A. Hassen, *Physica B* **499**(15), 24 (2016).
- ³¹A. Hassen, A. M. El Sayed, W. M. Morsi, and S. El-Sayed, *J. Appl. Phys.* **112**, 093525 (2012).
- ³²A. M. El Sayed, S. El-Sayed, W. M. Morsi, S. Mahrous, and A. Hassen, *Polym. Compos.* **35**(9), 1842 (2014).
- ³³N. F. Mott and E. A. Davis, *Electronic Process in Non-Crystalline Materials*, 2nd ed. (Oxford University Press, 1979), p. 273.
- ³⁴J. Tauc, *Optical Properties of Solid*, edited by A. Abeles (North Holland, Amsterdam, 1972), p. 277.
- ³⁵F. Urbach, *Phys. Rev.* **92**, 1324 (1953).